PHYSICAL REVIEW A VOLUME 35, NUMBER 2 JANUARY 15, 1987

Moments of the probability distribution for noisy maps

Jeffrey B. Weiss
Physics Department, University of California, Berkeley, California 94720
(Received 22 May 1986)

The effect of small-amplitude additive Gaussian white noise on maps with periodic attractors is studied. An expansion in powers of the mean-square noise strength is derived for the moments of the conditional probability distribution of position. The results are compared to numerical simulations of the logistic and Hénon maps, and agree to within the numerical uncertainty.

I. INTRODUCTION

It is impossible, and often undesirable, to completely isolate a physical system from its surroundings. Many new phenomena may appear due to the coupling of a system to a fluctuating environment;[1-10] noise-induced phase transitions can result, hopping between metastable states may occur, chaos may appear in parameter regimes which previously had regular motion, and the power spectrum of the motion exhibits precursors to instabilities. The primary effect of noise is that it causes the system to jump between neighboring trajectories. The net effect of successive jumps depends on the global flow of trajectories in phase space. In a chaotic system, where nearby trajectories diverge exponentially, noise merely adds to the divergence of neighboring initial conditions. When a trajectory passes near a separatrix between two regions of phase space, noise can drive the system across the separatrix, often resulting in qualitatively different behavior. If the system has a stable trajectory, the nearby trajectories approach the stable trajectory, and the noisy system will remain near, but not on, the deterministic trajectory, thus allowing one to express the motion of the noisy system in terms of properties of the deterministic trajectory. Stable periodic orbits have the advantage that the information required from the deterministic trajectory is contained in a finite time interval. For this reason, we focus on systems with stable periodic trajectories.

Dynamical systems can either be modeled by differential equations expressing the rate of change of the coordinates as a function of the present coordinates and time, or discrete maps relating the coordinates of the system to its coordinates at some previous time. Discrete maps are simpler to iterate numerically, and are often easier to study analytically. A discrete map can be constructed from a continuous trajectory by taking a Poincaré section.[11] This technique focuses on the intersection of the trajectory with a manifold having one less dimension than the phase space. A return map is constructed which relates the position on the manifold of each intersection in a prescribed sense to the position of the preceding intersection. Since the solution of a differential equation is unique, the resulting return map must be invertible. Discrete maps have been successfully used to study a wide variety of systems, including Josephson junctions,[12,13] nonlinear circuit elements,[14,15] and biological systems.[16] We take as our starting point a dynamical system described by a discrete map.

The unique trajectory $x(t)$ generated by an initial condition $x(0)$ in a deterministic system must be replaced in a noisy system by a conditional probability distribution $P(x(t) \mid x(0))$. A distribution function can be constructed for a deterministic system by either averaging over an ensemble of initial conditions, or averaging over a single ergodic trajectory.[17,18] Random noise is generally divided into two classes:[1] additive noise, in which stochastic terms independent of the state of the system are added to the equations of motion, and multiplicative noise, in which the noise terms depend on the state of the system. In the following, fluctuations will be modeled using additive Gaussian white noise. At each iteration of the map, the coordinates are given a random kick with Gaussian distributed amplitudes; successive kicks are independent of one another. Gaussian white noise is an appropriate approximation when the noise fluctuates on a time scale much faster than the response of the system.[19]

We imagine starting an ensemble of systems on a periodic attractor of the deterministic map, and allow them to evolve under the same map perturbed by noise. For sufficiently weak noise there is a separation of time scales. On a very fast time scale, the initial δ-function probability distribution evolves to a stationary distribution resulting from the balance between noise-induced diffusion and deterministic contraction onto the attractor. This stationary distribution is metastable, since, on a long time scale, systems in the ensemble will escape the basin of attraction of the initial attractor. Depending on the global structure of phase space, such a system will relax onto either the same attractor, possibly out of phase with the original motion, or onto a completely different attractor. The final equilibrium state will consist of localized probability distributions in each of the basins of attraction of the map. These localized pieces are the metastable distributions for each basin, weighted by the probability of a basin being occupied. In this paper we focus on the first stage of this process, and calculate moments of the probability distribution as it relaxes to the metastable equilibrium.

The analytic theory is outlined below. A map is constructed giving $\epsilon(t)$, defined as the deviation of the noisy trajectory from the deterministic attractor as a function of $\epsilon(t)$ one period earlier. This map is an expansion in

powers of the mean-square noise strength κ and depends on properties of the deterministic attractor and the particular noise realization. Averaging over the noise in ϵ, ϵ^2, etc., results in a map for the moments of the conditional probability distribution. To first order in the noise strength, one obtains a coupled pair of maps for the time evolution of the first two moments of the probability distribution. This set of maps can be solved analytically, resulting in an expression for the mean and variance of the probability distribution at times equal to an integer number of periods after the initial condition. Keeping terms of order κ^n results in $2n$ coupled maps for the first $2n$ moments.

The analytic calculation is tested against measurements of the moments of a numerically generated probability distribution for the logistic and Hénon maps. Both the logistic map,[16,20]

$$x(t+1)=rx(t)[1-x(t)], \quad 0<r\leq 4 \tag{1}$$

and the Hénon map,[21]

$$\begin{aligned} x(t+1)&=1+y(t)-ax^2(t)\ , \\ y(t+1)&=bx(t)\ , \end{aligned} \tag{2}$$

contain period-doubling cascades to chaos, providing attractors of period 2^n on which to study the probability distribution. In addition, attractors with odd period can be found within the chaotic regime. The bifurcation diagrams for the logistic and Hénon maps are shown in Figs. 1 and 2. Any numerical measurement must necessarily be over a finite-sized ensemble, and thus successive averages will not give identical results. It is found that an ensemble which is large enough to determine the variance of the probability distribution very precisely is too small to provide much information on the distribution's mean. In fact, for a period-two attractor in the logistic map, it is extrapolated that an ensemble of sufficient size to reduce the relative uncertainty in the mean to 1% would require five months of computation time on an IBM 3081. The discrepancy between analytic and numerical results is consistently within the numerical uncertainty. Thus we have a situation where the analytic theory predicts two quantities, only one of which is numerically accessible.

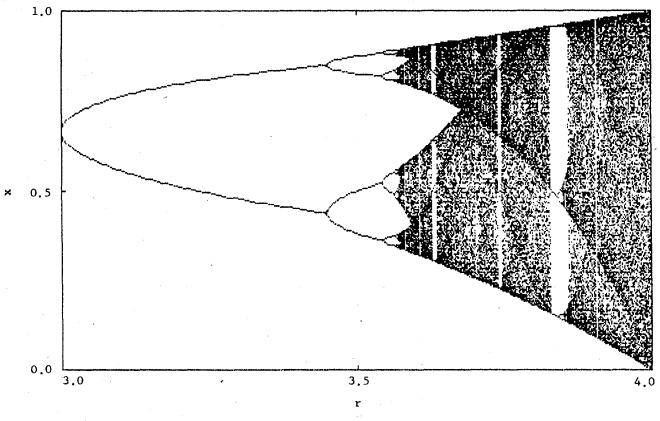

FIG. 1. Bifurcation diagram for the logistic map showing the attractor vs the parameter r. Two hundred iterations are plotted for each r in intervals of 0.002.

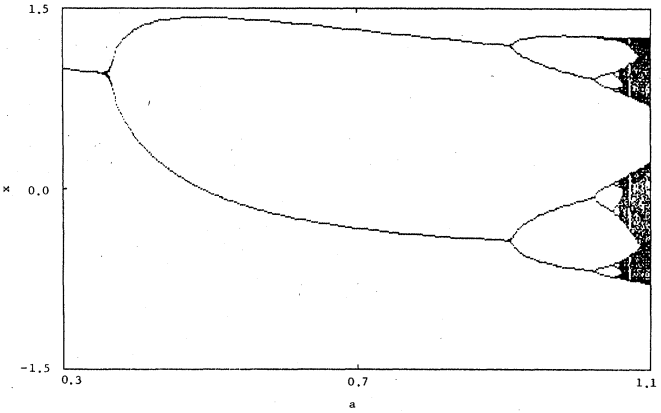

FIG. 2. Bifurcation diagram for the Hénon map showing the projection of the attractor onto the x axis vs the parameter a, for $b=0.3$. Two hundred iterations are plotted for each a in intervals of 0.0015.

II. ANALYTIC ANALYSIS

Consider a deterministic dynamical system governed by the map

$$x(t)=f(x(t-1);r), \quad x(t)\in \mathbb{R}^N, \ r\in \mathbb{R}^M\ . \tag{3}$$

The parameters r are assumed to be in a region where the map has a stable periodic attractor of period τ, A_τ, composed of τ phase points $\omega(s)$:

$$A_\tau=\{\omega(s)\mid \omega((s+1)\ (\mathrm{mod}\,\tau))=f(\omega(s);r)\}\ . \tag{4}$$

Repeated iteration of the map will be denoted by superscripts; $f\circ f\equiv f^2$, etc. Define the Jacobian matrix of t iterations of f evaluated on A_τ as $J^t_{\alpha\beta}(s)$:

$$J^t_{\alpha\beta}(s)\equiv \begin{cases} \delta_{\alpha\beta}, & t=0 \\ \left.\dfrac{\partial f^t_\alpha(x)}{\partial x_\beta}\right|_{x=\omega(s)}, & t>0 \end{cases} \tag{5}$$

where Greek subscripts denote components in $\mathbb{R}^N$. For each phase point of A_τ there is an $N\times N$ matrix of right eigenvectors, $V(s)$, which diagonalizes $J^\tau(s)$:

$$V^{-1}(s)J^\tau(s)V(s)=\begin{bmatrix} \lambda_1 & & 0 \\ & \ddots & \\ 0 & & \lambda_N \end{bmatrix}. \tag{6}$$

The eigenvectors depend on the phase point, while the eigenvalues λ_i do not. The eigenvalues measure the local stretching of lengths along their respective eigenvectors over a single period. A_τ is linearly stable if and only if there is a net contraction along all eigenvectors, i.e., all N eigenvalues of J^τ have modulus less than one. At individual phase points, however, the map may either stretch or contract intervals. A relationship between the eigen-

vectors at succeeding phase points is obtained using the identity

$$J^t(s)\equiv J^{t-u}((u+s)\ (\mathrm{mod}\,\tau))J^u(s),\quad 0\le u\le t \tag{7}$$

and Eq. (6):

$$V(s+1)=J^1(s)V(s)\ . \tag{8}$$

Thus the Jacobian of f at each phase point transforms the eigenvectors at that phase point into the eigenvectors at the next phase point.

The map is now perturbed by small mean-square amplitude Gaussian white noise $\xi(t)\in\mathbb{R}^N$ with probability distribution P_ξ:

$$y(t)=f(y(t-1);r)+\xi(t-1)\ , \tag{9}$$

where

$$\langle\xi_\alpha(t)\rangle=0,\quad \langle\xi_\alpha(s)\xi_\beta(t)\rangle=\kappa_{\alpha\beta}\delta_{s,t},\quad \kappa_{\alpha\beta}\ll 1\ . \tag{10}$$

The noisy trajectory will be denoted by $y(t)$, while the deterministic trajectory with identical initial condition will be labeled by $x(t)$. Define $\epsilon(t)$ as the difference between the noisy and deterministic trajectories: $\epsilon(t)\equiv y(t)-x(t)$. For a single noise realization with initial condition $y(0)$, the noisy trajectory is given by $y(t)=T(y(0),\xi)$, where

$$T(y(0),\xi)\equiv\xi(t-1)+f(\xi(t-2)+f(\xi(t-3)+\cdots+f(\xi(0)+f(y(0)))\cdots))\ . \tag{11}$$

The conditional probability distribution is obtained by averaging over noise realizations:[22]

$$P(y(t)\,|\,y(0))=\int d\xi(0)\cdots d\xi(t-1)P_\xi(\xi(0))\cdots P_\xi(\xi(t-1))\delta(y(t)-T(y(0),\xi))\ , \tag{12}$$

and satisfies the Chapman-Kolmogorov equation

$$P(y(t)\,|\,y(0))=\int dy(s)P(y(t)\,|\,y(s))P(y(s)\,|\,y(0))\ . \tag{13}$$

The moments of $P(y(t)\,|\,y(0))$ centered on $x(t)$ are defined by

$$M^n_{\alpha_1\cdots\alpha_n}(t,y(0))\equiv\int dy(t)\epsilon_{\alpha_1}(t)\cdots\epsilon_{\alpha_n}(t)P(y(t)\,|\,y(0))\ . \tag{14}$$

For an initial condition on A_τ, the contraction of the map will keep the noisy trajectory close to the deterministic one, and $\epsilon(t)$ will be small. Let $x(0)=y(0)=\omega(0)$; then the deterministic trajectory is given by $x(t)=\omega((t)\,(\mathrm{mod}\,\tau))$. It is convenient to work in a coordinate basis where $J^\tau(0)$ is diagonal;

$$x'=V^{-1}(0)x,\quad f'(x')=V^{-1}(0)f(V(0)x'),\quad J^{t\prime}(s)=V^{-1}(0)J^t(s)V(0),\quad \kappa'=V^{-1}(0)\kappa[V^{-1}(0)]^T\ . \tag{15}$$

In the following, we shall drop the primes. Equation (9) can be Taylor expanded about the deterministic trajectory, resulting in a map for $\epsilon(t)$ which depends on the properties of the map along the deterministic trajectory:

$$\epsilon_\alpha(t)=\xi_\alpha(t-1)+\sum_\beta\left.\frac{\partial f_\alpha}{\partial x_\beta}\right|_{\omega((t-1)\,(\mathrm{mod}\,\tau))}\epsilon_\beta(t-1)+\tfrac{1}{2}\sum_{\beta,\gamma}\left.\frac{\partial^2 f_\alpha}{\partial x_\beta\partial x_\gamma}\right|_{\omega((t-1)\,(\mathrm{mod}\,\tau))}\epsilon_\beta(t-1)\epsilon_\gamma(t-1)+\cdots\ . \tag{16}$$

A map for $\epsilon(t)$ over one period can be obtained by repeated iteration of Eq. (16) along with Eqs. (5) and (7):

$$\epsilon_\alpha(t)=\xi_\alpha(t-1)+\sum_{s=1}^{\tau-1}\left[\sum_\beta J^s_{\alpha\beta}(\tau-s)\xi_\beta(t-s-1)+\sum_{\beta,\gamma}L_{\alpha\beta\gamma}(\tau-s)\xi_\beta(t-s-1)\xi_\gamma(t-s-1)\right]$$
$$+\lambda_\alpha\epsilon_\alpha(t-\tau)+\sum_{\beta,\gamma}L_{\alpha\beta\gamma}(0)\epsilon_\beta(t-\tau)\epsilon_\gamma(t-\tau)+\cdots\ , \tag{17}$$

where

$$L_{\alpha\beta\gamma}(s)\equiv\tfrac{1}{2}\sum_{r=s}^{\tau-1}\sum_{\rho,\mu,\nu}J^{\tau-r-1}_{\alpha\rho}(r+1)\left.\frac{\partial^2 f_\rho}{\partial x_\mu\partial x_\nu}\right|_{\omega(r)}J^{r-s}_{\mu\beta}(s)J^{r-s}_{\nu\gamma}(s)\ . \tag{18}$$

The higher-order terms left out of Eq. (17) are those which, when M^1 and M^2 are calculated, are either identically zero or $O(\kappa^2)$.

We now focus on $\epsilon(t)$ at times equal to an integer number of periods: $t=m\tau$. Since $\epsilon(0)=0$, and Eq. (17) contains no terms independent of both ξ and ϵ, the moments depend on the noise strength in the following manner:

$$M^{2n-1}\sim M^{2n}\sim O(\kappa^n)\ . \tag{19}$$

Using Eqs. (10), (12), and (13), one can explicitly average over the noise in Eq. (17) from time $(m-1)\tau$ through time $m\tau-1$ to obtain

$$M^1_\alpha(m\tau)=\lambda_\alpha M^1_\alpha((m-1)\tau)+\sum_{\beta,\gamma}L_{\alpha\beta\gamma}(0)M^2_{\beta\gamma}((m-1)\tau)+B_\alpha+O(\kappa^2),$$
$$M^2_{\alpha\beta}(m\tau)=\lambda_\alpha\lambda_\beta M^2_{\alpha\beta}((m-1)\tau)+C_{\alpha\beta}+O(\kappa^2)\ , \tag{20}$$

where

$$B_\alpha \equiv \sum_{s=1}^{\tau-1} \sum_{\beta,\gamma} L_{\alpha\beta\gamma}(\tau-s)\kappa_{\beta\gamma} ,$$
$$C_{\alpha\beta} \equiv \kappa_{\alpha\beta} + \sum_{s=1}^{\tau-1} \sum_{\gamma,\delta} J^s_{\alpha\gamma}(\tau-s) J^s_{\beta\delta}(\tau-s)\kappa_{\gamma\delta} . \tag{21}$$

If terms which average to $O(\kappa^n)$ are kept in Eq. (17), a coupled set of maps for the first $2n$ moments results. Equation (20) can be solved exactly for all m. Using the initial condition $M^1(0)=M^2(0)=0$, one obtains

$$M^1_\alpha(m\tau) = \sum_{\beta,\gamma} \frac{L_{\alpha\beta\gamma}(0)C_{\beta\gamma}}{1-\lambda_\beta\lambda_\gamma} \times \left[\frac{1-\lambda_\alpha^{m-1}}{1-\lambda_\alpha} - \frac{(\lambda_\beta\lambda_\gamma)^m - \lambda_\alpha^{m-1}\lambda_\beta\lambda_\gamma}{\lambda_\beta\lambda_\gamma - \lambda_\alpha} \right] + \frac{1-\lambda_\alpha^m}{1-\lambda_\alpha} B_\alpha + O(\kappa^2) ,$$
$$M^2_{\alpha\beta}(m\tau) = \frac{1-(\lambda_\alpha\lambda_\beta)^m}{1-\lambda_\alpha\lambda_\beta} C_{\alpha\beta} + O(\kappa^2) . \tag{22}$$

The moments of the metastable equilibrium distribution can be obtained from either the fixed point of Eq. (20), or letting $m \to \infty$ in Eq. (22):

$$M^1_\alpha(\text{eq}) = \frac{B_\alpha}{1-\lambda_\alpha} + \sum_{\beta,\gamma} \frac{L_{\alpha\beta\gamma}(0)C_{\beta\gamma}}{1-\lambda_\beta\lambda_\gamma} + O(\kappa^2) ,$$
$$M^2_{\alpha\beta}(\text{eq}) = \frac{C_{\alpha\beta}}{1-\lambda_\alpha\lambda_\beta} + O(\kappa^2) . \tag{23}$$

Notice that Eq. (22) converges to Eq. (23) as $m \to \infty$ only if $|\lambda_\alpha| < 1$ for all α. This is also the condition for stability of both the fixed point of Eq. (20), and the attractor A_τ itself. Thus, when A_τ is unstable, the moments diverge.

III. NUMERICAL SIMULATIONS

The results of the previous section are compared with numerical iteration of Eq. (9) for both the logistic map, Eq. (1), and the Hénon map, Eq. (2). Figures 1 and 2 depict the bifurcation diagrams for the logistic and Hénon maps, respectively. Both maps exhibit a period-doubling cascade to chaos with periodic windows in the chaotic regime, providing periodic attractors on which to test the theory. The numerical moments are measured in the original coordinates of the map, while the analytic results are given in the eigenbasis defined by Eq. (15). Since the logistic map is one dimensional, no coordinate change is necessary. For the Hénon map, however, the moments given by Eqs. (22) and (23) are transformed back into the original coordinates to compare with the numerical results.

The numerical calculations are done in double precision on an IBM 3081 mainframe computer. Twenty independent pseudorandom numbers, evenly distributed over an interval, are added together to approximate a pseudorandom Gaussian distributed variable whose mean-square noise strength is determined by the length of the interval. The convergence to Gaussian noise and the relation between the length of the interval and the mean-square noise strength are given by the central-limit theorem.[23] The mean-square noise strengths used are $\kappa = 10^{-10}$ for the logistic map, and $\kappa_{\alpha\beta} = 10^{-10}\delta_{\alpha\beta}$ for the Hénon map.

The equilibrium moments are discussed first. Motion within the metastable distribution is assumed to be ergodic, and the equilibrium moments are thus calculated by averaging over a single trajectory. For any finite time interval, successive averages will differ from both each other and the analytic result. The convergence of the numerical measurement is indicated by the rms deviation of successive averages over equal times and with identical initial conditions. The equilibrium moments are calculated as follows: the trajectory is iterated for 200 periods to allow any initial transient to decay, after which an average is taken over ten groups of 10^6 periods each. Table I shows the results for attractors of various periods in the logistic map. The analytic result consistently falls within the numerical uncertainty. Most striking, however, is the poor convergence of M^1 compared to M^2: the uncertainty for M^1 is in the first digit, while for M^2 it is in the third or fourth digit. Thus M^2 can be measured very precisely in 10^6 periods, while M^1 is almost completely undetermined. While the relative uncertainty of both moments follows the usual power law, $\Delta M_{\text{rms}}/M \propto (\text{periods averaged})^{-1/2}$, the proportionality constant for M^1 is 10^4 times that for M^2. Reducing the relative uncertainty of M^1 to 1% would require roughly five months of CPU time. The Hénon map shows a similar slow convergence of M^1. Thus in order to test the analytic theory against numerical simulations, we ignore M^1 and focus solely on M^2.

We next study the decay of a δ-function probability distribution centered on a phase point of the deterministic attractor. The decay of the moments is given analytically

TABLE I. Comparison of analytic and numerical calculations of the mean, M^1, and variance, M^2, of the equilibrium distribution for various parameters r in the noisy logistic map with noise strength $\kappa = 10^{-10}$.

r	Period	Analytic M^1/κ M^2/κ	Numerical $M^1/\kappa \pm \Delta M^1_{\text{rms}}/\kappa$ $M^2/\kappa \pm \Delta M^2_{\text{rms}}/\kappa$
2.00	1	−2.00	−27.43±78.24
		1.000	1.000±0.002
3.20	2	31.1	69.1±127.5
		4.796	4.795±0.004
3.50	4	−524	−365±546
		34.08	34.05±0.03
3.554	8	9400	9519±1886
		227.4	227.4±0.3
3.831 874	3	33057	33377±9488
		94.5	94.5±0.1

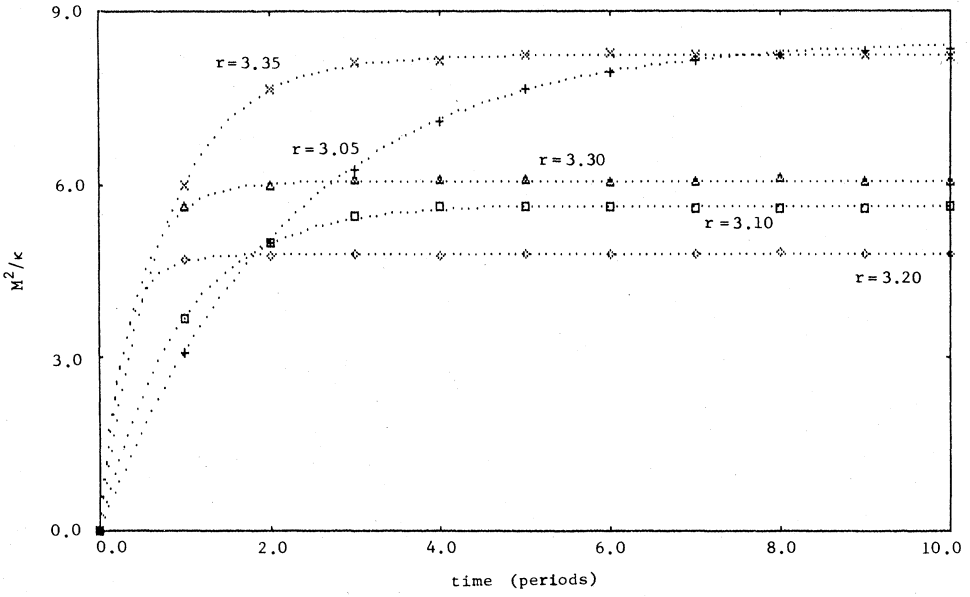

FIG. 3. Comparison of analytic and numerical measurements of M^2/κ vs time for the logistic map in the period-two regime. The initial condition is a δ-function distribution on the deterministic attractor. The symbols are numerical measurements and the dotted lines are continuous interpolation of Eq. (22).

by Eq. (22). The numerical calculation is done by averaging over 10^5 trajectories starting on the attractor. Figures 3 and 4 compare the analytic and numerical results for M^2 for various parameter values in the period-two and period-four regimes of the logistic map. Figure 5 is a similar comparison of M_{xx}^2 for the period-two regime of the Hénon map. Although Eq. (22) is strictly valid only for integer values of m, fractional values are plotted to facilitate comparison. The results show excellent agreement between the analytic theory and numerical simulations. As the parameter in the logistic map progresses through a regime of a given period, the eigenvalue of the attractor evolves from positive one through zero to negative one, where a period-doubling bifurcation occurs. Equation

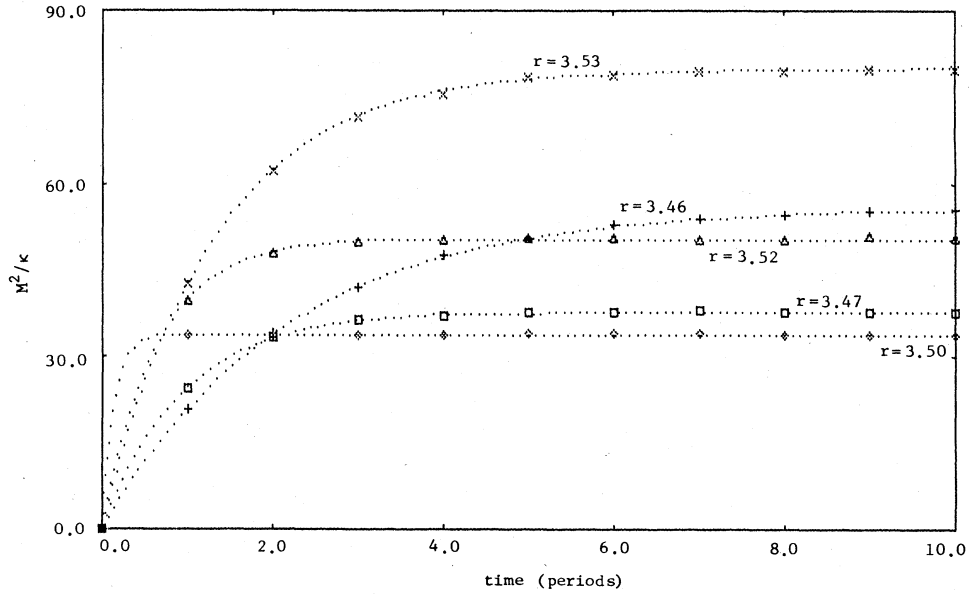

FIG. 4. Same as Fig. 3, except for parameter values in the period-four regime.

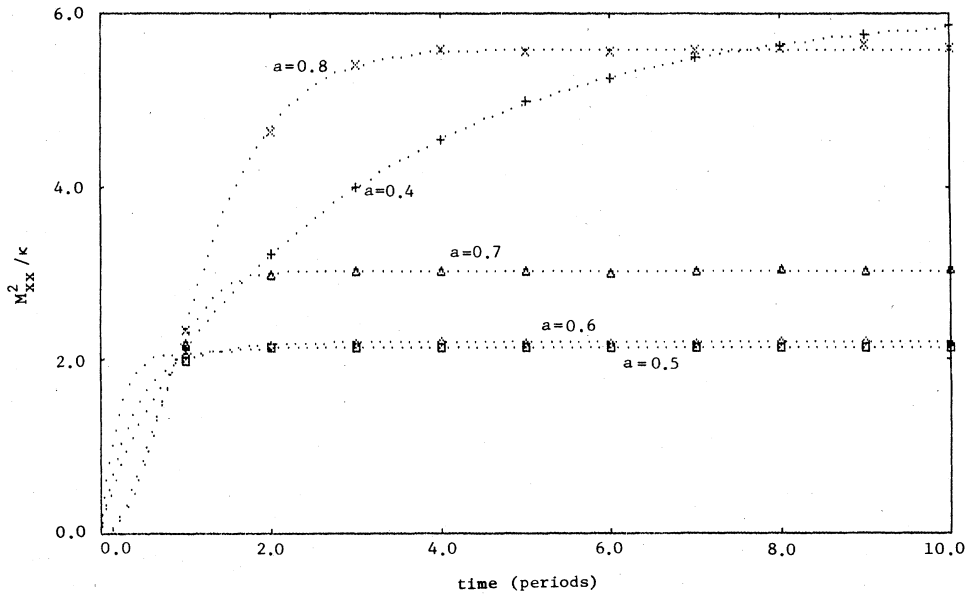

FIG. 5. Same as Fig. 3, except M^2_{xx}/κ is plotted for the Hénon map in the period-two regime.

(23) thus predicts the dependence of M^2(eq) on r seen in Figs. 3 and 4: as r increases through a periodic regime M^2(eq) first decreases and then increases. Similar behavior occurs in the Hénon map (Fig. 5) for basically the same reason, although small complications do arise from the two-dimensional nature of the map.

Given the above results, it is natural to ask how well the metastable equilibrium distribution is approximated by the Gaussian constructed from M^1 and M^2. Motion within the equilibrium distribution is again assumed to be ergodic, and a histogram is constructed by placing 10^5 iterations of the logistic map at $r=3.525$ into 100 bins from $x=0.5143$ to $x=0.5149$. The phase point of the period-two attractor is at $x\simeq 0.514\,614$. Figure 6 shows

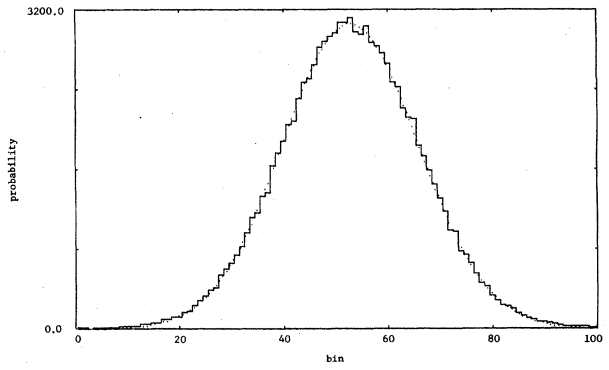

FIG. 6. Unnormalized probability distribution for the logistic map with $r=3.525$ around the phase point $x\simeq 0.514\,614$. The histogram shows the result for 10^5 iterations placed into 100 bins from $x=0.5143$ to $x=0.5149$. The dotted line is a Gaussian distribution with mean and variance given by Eq. (23).

that the equilibrium distribution is, in fact, quite close to a Gaussian with moments given by Eq. (23).

IV. CONCLUSION

It is possible to calculate the moments of the conditional probability distribution for an iterated map with a stable periodic orbit perturbed by small-amplitude additive Gaussian white noise. The moments decay to their equilibrium values in a small number of periods, and remain there for times on the order of the mean first-passage time of the system. The metastable equilibrium distribution is well approximated by a Gaussian with moments given by the theory. The analytic calculation for the variance of the distribution agrees with the numerical simulations to within the numerical uncertainty, roughly 0.1%. The mean of the distribution is numerically inaccessible due to slow convergence of the average. The analytic theory thus provides more information than is possible to obtain by direct numerical iteration of the map.

In much of the work on the mean first-passage time, one starts with assumptions about the metastable distribution.[24–26] The above work should provide a basis for the calculation of the mean first-passage time for maps with stable periodic orbits.

ACKNOWLEDGMENTS

The author would like to thank D. Clegg, J. Lerner, and especially E. Knobloch for many useful discussions. This work was supported in part by the California Space Institute and the IBM Distributed Academic Computing Environment (DACE) grant.

[1]W. Horsthemke and R. Lefever, *Noise-induced Transitions: Theory and Applications in Physics, Chemistry, and Biology* (Springer-Verlag, Berlin, 1984).
[2]*Fluctuations and Sensitivity in Nonequilibrium Systems,* edited by W. Horsthemke and D. K. Kondepudi (Springer-Verlag, Berlin, 1984).
[3]S. Fraser, E. Celarier, and R. Kapral, J. Stat. Phys. **33**, 341 (1983).
[4]J. P. Crutchfield and B. A. Huberman, Phys. Lett. **77A**, 407 (1980).
[5]J. Crutchfield, M. Nauenberg, and J. Rudnick, Phys. Rev. Lett. **46**, 933 (1981).
[6]J. P. Crutchfield, J. D. Farmer, and B. A. Huberman, Phys. Rep. **92**, 45 (1982).
[7]G. Meyer-Kress and H. Haken, J. Stat. Phys. **26**, 149 (1981).
[8]K. Wiesenfeld, J. Stat. Phys. **38**, 1071 (1985).
[9]C. Jeffries and K. Wiesenfeld, Phys. Rev. A **31**, 1077 (1985).
[10]B. Shraiman, C. E. Wayne, and P. C. Martin, Phys. Rev. Lett. **46**, 935 (1981).
[11]J. Guckenheimer and P. Holmes, *Nonlinear Oscillations, Dynamical Systems, and Bifurcations of Vector Fields* (Springer-Verlag, New York, 1983).
[12]R. F. Miracky, M. H. Devoret, and J. Clarke, Phys. Rev. A **31**, 2509 (1985).
[13]M. H. Jensen, P. Bak, and T. Bohr, Phys. Rev. A **30**, 1960 (1984).
[14]J. Perez and C. Jeffries, Phys. Lett. **92A**, 82 (1982).
[15]C. Jeffries and J. Perez, Phys. Rev. A **26**, 2117 (1982).
[16]R. M. May, Nature (London) **261**, 459 (1976).
[17]H. D. J. Abarbanel and P. E. Latham, Phys. Lett. **89A**, 55 (1982).
[18]S. Chang and J. Wright, Phys. Rev. A **23**, 1419 (1981).
[19]R. L. Stratonovich, *Topics in the Theory of Random Noise* (Gordon and Breach, New York, 1963), Vol. 1.
[20]M. J. Feigenbaum, J. Stat. Phys. **19**, 25 (1978).
[21]M. Hénon, Commun. Math. Phys. **50**, 69 (1976).
[22]H. Haken and G. Meyer-Kress, Phys. Lett. **84A**, 159 (1981); Z. Phys. B **43**, 185 (1981).
[23]A. I. Khinchin, *Mathematical Foundations of Statistical Mechanics* (Dover, New York, 1949).
[24]H. A. Kramers, Physica **7**, 284 (1940).
[25]B. J. Matkowsky, Z. Schuss, C. Knessl, C. Tier, and M. Mangel, Phys. Rev. A **29**, 3359 (1984).
[26]D. Ryter, Physica **130A**, 205 (1985).